THE EUROSDR PROJECT "RADIOMETRIC ASPECTS OF DIGITAL PHOTOGRAMMETRIC IMAGES" – RESULTS OF THE EMPIRICAL PHASE

E. Honkavaara [a, *], R. Arbiol [b], L. Markelin [a], L. Martinez [b], S. Bovet [c], M. Bredif [d], L. Chandelier [e], V. Heikkinen [f], I. Korpela [g], L. Lelegard [d], F. Pérez[b], D. Schläpfer [h], T. Tokola [f]

[a] Finnish Geodetic Institute, Geodeetinrinne 2, P.O. Box 15, FI-02431 Masala, Finland – (eija.honkavaara, lauri.markelin)@fgi.fi
[b] Institut Cartografic de Catalunya. Parc de Montjuïc s/n 08038 Barcelona (Spain) – (roman.arbiol, lucas.martinez, fernando.perez)@icc.cat
[c] Swisstopo - Land survey of Switzerland, Seftigenstrasse 264, CH 3084 Wabern, Switzerland – (stephane.bovet)@swisstopo.ch
[d] Institut Géographique National (IGN), 2-4 avenue Pasteur 94165 SAINT MANDE CEDEX, France – (mathieu.bredif, laman.lelegard)@ign.fr
[e] Ecole Nationale des Sciences Géographiques (ENSG), 6, et 8 avenue Blaise Pascal - Cité Descartes - Champs-sur-Marne, 77455 Marne la Vallée Cedex 2, France – (laure.chandelier)@ensg.eu
[f] Faculty of Natural and Forest Sciences, University of Eastern Finland, Joensuu, 80101 Finland, – (ville.heikkinen, timo.tokola)@uef.fi
[g] Faculty of Agriculture and Forestry, Department of Forest Resource Management, University of Helsinki, Helsinki, 00014 Finland, – (ilkka.korpela)@helsinki.fi
[h] ReSe Applications Schlaepfer, Langeggweg 3, CH-9500 Wil, Switzerland – (info)@rese.ch

Commission VI, WG VI/4

KEY WORDS: Atmospheric correction, calibration, radiometry, resolution, reflectance, photogrammetry

ABSTRACT:

This article presents the empirical research carried out in the context of the multi-site EuroSDR project "Radiometric aspects of digital photogrammetric images" and provides highlights of the results. The investigations have considered the vicarious radiometric and spatial resolution validation and calibration of the sensor system, radiometric processing of the image blocks either by performing relative radiometric block equalization or into absolutely reflectance calibrated products, and finally aspects of practical applications on NDVI layer generation and tree species classification. The data sets were provided by Leica Geosystems ADS40 and Intergraph DMC and the participants represented stakeholders in National Mapping Authorities, software development and research. The investigations proved the stability and quality of evaluated imaging systems with respect to radiometry and optical system. The first new-generation methods for reflectance calibration and equalization of photogrammetric image block data provided promising accuracy and were also functional from the productivity and usability points of view. The reflectance calibration methods provided up to 5% accuracy without any ground reference. Application oriented results indicated that automatic interpretation methods will benefit from the optimal use of radiometrically accurate multi-view photogrammetric imagery.

1. INTRODUCTION

The special advantage of the new digital large-format photogrammetric imagery is the high-quality multi-spectral radiometry. The high-quality radiometry opens up new prospects for the utilization of the photogrammetric imagery, but also requires new approaches for the data processing. Accurate radiometric processing is necessary for both visual and quantitative applications. The rigorous treatment of the image radiometry is a new issue in photogrammetric processing lines.

To investigate these issues, the EuroSDR launched a project called "Radiometric aspects of digital photogrammetric images" in May 2008.

The first phase of the project consisted of a literature review and a questionnaire (Honkavaara et al., 2009). The major conclusions of the questionnaire were that improvements were requested for the entire process: sensors, calibration, data collection, data post-processing and data utilization. The fundamental problems could be listed as follows: there was insufficient information of the radiometric processing chain, radiometric processing lines were inadequate and standards were missing (methods, calibration, reference targets, and terminology). The basic radiometric end products requested by image users were true color images and reflectance images. The expected benefits of a more accurate radiometric processing include a more automatic and efficient image post-processing, better visual image quality, more accurate and automatic interpretation, and the remote sensing use of data.

Based on the results of the questionnaire and the potential of the available image materials, the following topics were selected as the general objectives of the empirical phase of the project:
1. Radiometric calibration and characterization
2. Spatial resolution assessment

---
* Corresponding author.

3. Reflectance calibration and image block equalization
4. Colour enhancement of the calibrated data
5. Application oriented studies

These topics cover the very fundamental processes of the radiometric processing line. The first two objectives are related to validation and calibration of the imaging sensor and system, which should be carried out on a regular basis (e.g. yearly) to ensure the quality of the imaging system. These aspects should be considered also in the acceptance testing of a purchased new sensor system. Objectives 3 and 4 are related to the processing of huge amounts of image data (tens to hundreds of thousands of km^2 every year). The key requirements for these processes include efficiency (fast processing, no ground reference targets), usability aspects (simplicity of use, automatic selection of parameters), reliability and accuracy. The last objective is related to the fact that the radiometric processing level and quality of image data has influences in applications.

The objective of this paper is to present the research carried out in the context of the EuroSDR project and to present the main results. In Section 2 the empirical data sets, participants and processing methods are briefly described. Section 3 provides some highlights of the results and conclusions are given in Section 4.

2. EMPIRICAL INVESTIGATION

2.1 Empirical image data

In summer/autumn 2008 radiometrically controlled test flights were conducted in Catalonia (Spain) and Finland.

2.1.1 Integrated DMC and CASI test flight in Banyoles. The Institut Cartogràfic de Catalunya (ICC) executed extensive radiometric test flights with a DMC camera and a Compact Airborne Spectrographic Imager (CASI) in Banyoles on 15 July, 2008 (Arbiol and Martinez, 2009). The imagery was collected at 820, 1125, 2250 and 4500 m flying heights above the ground. Various manmade reflectance targets as well as several artificial and natural stable covers were available around the test field, including a lake. In addition, a Siemens star was installed in the test field. Two groups carried out the radiance and reflectance ground-truth data acquisition with spectroradiometers. The atmospheric state was directly measured by several groups, instruments and techniques. An atmospheric Lidar provided aerosol profiles and two automatic sun tracking photometers provided column integrated values of Aerosol Optical Thickness (AOT) for the optical spectrum. Atmospheric profiles of the area were calculated for the campaign day from weather forecast models by the Catalonian weather service.

2.1.2 DMC test flights in Sjökulla. The National Land Survey of Finland carried out a acceptance test of their new DMC on 1 and 25 September 2008 at the Sjökulla test field of the Finnish Geodetic Institute (FGI) (Honkavaara et al., 2011). The flying height was 500 m above the ground level, which provided 5 cm GSD. The reflectance reference targets included the permanent bi-directional reflectance factor (BRF) targets of gravel at the test field, several transportable BRF targets and several natural reflectance targets; the targets were monitored using an ASD field spectrometer during the first flight. A Siemens star, an edge target and line bar targets were available for the spatial resolution evaluations. The special feature of this data was that it included several overflights with different exposure settings.

BRF-targets are needed, because the photogrammetric systems used have a wide field of view and the reflectance anisotropy has to be taken into account in evaluations. The anisotropic reflectance characteristics of the FGI reference targets have been measured in the laboratory using the FIGIFIGO goniospectrometer (Suomalainen et al., 2009). The reference values for different view/illumination geometries are obtained either by using these anisotropy factors to scale the nadir reflectance value measured in the field conditions or the reference value is interpolated from BRF data measured in the laboratory.

2.1.3 Integrated ADS40/ALS50 test flight in Hyytiälä. The test flight with ADS40 (SH 52) and ALS50 was carried out at the Hyytiälä forestry test field in co-operation with Leica Geosystems, University of Helsinki, University of Eastern Finland, Estonian Land Board and FGI. The test site is 3300 m x 8500 m in size and it contains more than 200 forest plots in different forest conditions (density, age, species mixture, silvicultural history) with over 15000 trees that have been measured for position and basic variables (Korpela et al., 2011). Atmospheric and weather conditions were measured by the permanent SMEAR-II and AERONET stations that are in the area. FGI's BRF calibrated reflectance targets and a Siemens star were installed at the test field. The reflectance/radiance of the targets as well as various homogeneous land covers (asphalt, gravel, grass) were monitored by spectroradiometers. The ADS40 data was collected in uncompressed mode at 1000, 2000, 3000 and 4000 m flying altitudes providing 10 cm, 20 cm, 30 cm, and 40 cm GSD.

2.2 Participants

The participants of the empirical phase included three National Mapping Agencies (NMAs), one company providing atmospheric correction software and eight research participants. The data was delivered to some additional parties, but they did not return any results.

NMAs
- Institut Cartografic de Catalunya, Spain (ICC)
- Institut Géographique National, France: Ecole Nationale des Sciences Géographiques (IGN/ENSG) and Laboratoire MATIS (IGN/MATIS)
- Swisstopo, Switzerland

Software development
- ReSe, Switzerland

Research:
- Finland: FGI, University of Helsinki (UH), University of Eastern Finland (UEF)
- Spain: Instituto de Desarrollo Regional – Universidad de Castilla La Mancha (IDR-UCLM), Centre de Recerca Ecològica i Aplicacions Forestals – Universitat Autònoma de Barcelona (CREAF-UAB), Universitat de Barcelona (UB), Universitat Politècnica de Catalunya (UPC), Servei Meteorològic de Catalunya (SMC)

All participants are active in research, the IGN is developing their own camera and software, and the ICC is developing software, so the participants provided several points of view.

2.3 Processing of the data

The objectives of the empirical study were covered by the following participants, data sets and approaches:

Radiometric calibration and characterization
- CASI Banyoles by ICC (6S)
- DMC Banyoles by ICC
- DMC Sjökulla by FGI (Modtran 4)
- ADS40 Hyytiälä by ReSe (ATCOR-4) and by FGI (Modtran 4, ATCOR-4)

Spatial resolution assessment
- DMC Banyoles by IGN/MATIS
- DMC Banyoles by ICC
- DMC Sjökulla by FGI

Reflectance calibration, image block equalization
- DMC Banyoles by IGN/ENSG (Pepita)
- DMC Sjökulla by FGI (Modified empirical line)
- ADS40 Hyytiälä by ReSe (ATCOR-4), FGI (ATCOR-4 and XPro 4.2.0) and Swisstopo (XPro 4.2.0)

Application oriented evaluations
- DMC Banyoles: NDVI map production by ICC
- ADS40 Hyytiälä: tree species classification by UH and UEF

2.4 Radiometric calibration and characterization

The radiometric calibration and characterization were carried out using photogrammetric systems and a CASI hyper-spectral scanner. Reflectance and radiance based approaches were covered.

2.4.1 CASI Banyoles. The determination of the DMC radiometric calibration parameters was the main objective of the ICC's previous campaign in 2005 and obtained results were indeed satisfactory enough, but the secondary objective concerning the results of atmospheric correction of DMC images was disappointing. Without real measurements the obtained values could not be applied. Even worse, the hypothesis that the CASI could be used as a calibration system was far from reality due to a poor knowledge on the detailed response of the hyperspectral sensor.

The spectral shift characterization method is based on the hypothesis of global g-coefficients that need to be identically shifted for all the wavelengths for each look direction. The proposed methodology exploits the presence of the O_2 atmospheric absorption band (760 nm approx.) over a high reflectance cover in that wavelength. To determine the spectral shift, a non-orthorectified hyperspectral image over a vegetated area is aggregated in the along-track direction. This process generates a one-line image with 550 across-track spectral samples (look directions). Then, a subpixel Pearson correlation is computed for each one of the 550 spectra with a vegetation spectrum processed with the 6S code (Vermote et al., 1997) to take into account the effect of the O_2 absorption band. The estimated spectral shift is then applied to the original image and the radiometric bands are spectrally resampled to fit the CASI channel nominal limits described by the g-coefficients (Martinez et al., 2011).

The first approximation to the sensitivity of the bands was a rectangular response between the limits of each channel. This simple estimation works fine to correct from atmospheric scattering but proves insufficient to solve the absorption regions. The manufacturer was then asked about the sensitivity of the bands and we received a polynomial relationship between FWHM and wavelength that shows values up to several times the nominal FWHM of the sensor (Martinez et al.,2011).

2.4.2 DMC Banyoles. Vicarious radiance based radiometric calibration was carried out for the DMC by using simultaneous images of DMC and CASI. The CASI system is periodically recalibrated in the laboratory, and the idea was to transfer this calibration to the DMC. This is possible due to the fact that the acquisition geometry, atmospheric effects and illumination geometry of the targets are approximately equivalent for areas imaged simultaneously. Besides, the spectral resolution of CASI is high enough to reproduce DMC-like channels by adding calibrated CASI hyper-spectral bands. In order to verify the previous hypothesis and because of the different FOV of DMC and CASI, only the central area of the DMC scenes were used. In addition, DMC pixels were aggregated to fit the coarse CASI spatial resolution. Then a median floating window filter was applied to both CASI and DMC imagery to avoid misregistration and other sources of noise. Finally, a linear relationship between Digital Numbers (DN) from DMC and radiance values of a CASI image emulating DMC bands is derived (Martínez et al., 2007).

2.4.3 DMC Sjökulla. The reflectance based vicarious calibration was applied for the DMC images. The reflectance spectrums of several reference targets were measured during the campaign. The at-sensor radiances were then calculated using the Modtran 4 radiative transfer code. As insitu measurements of atmospheric conditions were not available, standard "Midlatitude summer" atmospheric settings were used. The images were collected using various exposure settings (aperture, exposure time), and the calibration was calculated using DNs that were normalized using the aperture and exposure time. The stability of the sensor was also evaluated. Details of the approach are given by Markelin et al. (2010a).

2.4.4 ADS40 Hyytiälä. An absolute radiometric calibration of the ADS40 was carried out using the reflectance based vicarious calibration method using ATCOR-4 (Schläpfer, 2010) and on at-sensor radiance level using Modtran 4 (Markelin et al., 2010b). Two reference targets were used in the latter calibration. In Modtran 4 radiative transfer calculations, the ground reflectance measurements and the atmospheric measurements of the SMEAR-II and AERONET stations were used. In ATCOR-4, the aerosol optical thickness was derived from the image data.

2.5 Spatial resolution assessment

2.5.1 DMC Banyoles. A Siemens star made of canvas of size of 100 m^2 and with 5° sectors was available at the test site. The target appeared in different positions on 9 DMC images from the lowest flying height.

The IGN/MATIS used the Siemens star to determine the MTFs. Furthermore, the local image sharpness was studied by using Haar Wavelets Transform (Brédif and Lelégard, 2010).

At the ICC, a software tool was implemented with the aim of providing a spatial resolution measurement of an image in pixel

units. The program processes a region of interest that contains a single contour and makes a minimum square adjustment over the bi-dimensional function of the edge that is modelled as a sigmoid function. The five parameters are estimated in a least squares adjustment and the computed function is derived for obtaining the LSF (Line Spread Function). The FWHM (Full Width at Half Maximum) over the LSF is the measurement value (Talaya et al., 2007). The image resolution loss caused by the atmosphere as a function of the atmospheric radiative conditions was analysed. The resolution in pixel units was evaluated as the FWHM of the LSF computed from a reconstruction of the Edge Spread Function (ESF). The 6S (Vermote et al., 1997) code was used to simulate the atmosphere. Atmosphere type, aerosol model and total load, illumination and observation geometries and spectral range are taken into account when computing simulations. The results were also compared with the resolution measures on the real images taken with the DMC.

2.5.2   DMC Sjökulla. For the FGI Sjökulla DMC data sets, a Siemens star and RP-targets were used for the resolution assessment. The resolution targets were spread over the image area on 35 positions on first acquisition day and on 18 positions on second acquisition day. The image resolution was analyzed as the function of radial distance from the image centre. Further evaluations were carried out to consider impacts of exposure settings on the resolution. The methods are described by Honkavaara et al. (2011).

2.6 Reflectance calibration and image block equalization

Several relevant approaches for reflectance calibration and image block equalization were tested in the study.

2.6.1   Pepita of IGN. The "radiometric aerial triangulation" Pepita software is a method for equalising a block of digital aerial images, which can be considered as relative radiometric calibration (Chandelier and Martinoty, 2008). It is based on a parametric, semi-empirical radiometric model taking into account BRDF, haze differences between blocks of images, solar elevation, sensor settings (exposure) and a optional radial component (mainly for chromatic aberration). The model parameters are computed through a global least-squares minimisation process, using radiometric tie-points in overlapping areas between the images. As a result, a relative equalisation between the images is obtained. The method has been used in the IGN orthoimage workflow since 2005. At the beginning, Pepita has only been tested and used on IGN-v1 camera images, giving satisfying results. In 2008, some tests were carried out on DMC images, but the results did not meet the requirements of the IGN orthoimage database specifications. In 2009, IGN acquired its own UltraCam XP camera and Pepita is currently used both on UXP and IGN-v2 cameras.

2.6.2   ATCOR-4 of Rese. The ATCOR-4 performs a physically based atmospheric/topographic correction for airborne scanner data in the solar (0.35-2.55 µm) and thermal (8-14 µm) spectral region. The correction is based on pre-calculated MODTRAN® look-up tables of the atmospheric radiation field (Richter 2010, Richter 2002). The output in the solar region is the surface reflectance cube and in the thermal region it is the surface (brightness) temperature and emissivity spectrum. The capabilities of the software include determination of the aerosol map (requires bands in the near infrared and/or in the short wave infrared region) and the spatial water vapor map (requires bands in the 940/1130 nm region), haze and cirrus cloud removal (low altitude haze) and inflight sensor calibration using ground reference targets. ATCOR-4 is for wide FOV airborne scanner imagery and for all terrain types, and it includes the capability for radiometric correction in rugged terrain with cast shadow and illumination calculations.

2.6.3   XPro of Leica Geosystems. Leica Geosystems XPro takes care of the entire post-processing workflow of the ADS-imagery from data download to the generation of stereo models and orthoimages. Main features from the radiometric point of view are the options to produce ground radiance and ground reflectance images. The default product of XPro is calibrated DN, which relates the pixel data to at-sensor radiances. There are two options to produce ground radiance data: the Dark Pixel Subtraction and the Modified Chavez methods. Ground radiances are still dependent on the illumination level and vary from flight line to flight line. Ground reflectances are calculated by dividing the reflected radiance by the incoming solar irradiance, which is estimated based on the radiative transfer equation by Fraser et al. (1992) and using a parameterization of the atmospheric parameters based on the method of Song et al. (2003). All three correction methods are based on an automatic dark object method to tune the corrections to the actual atmospheric conditions. Additionally, BRDF (Bidirectional reflectance distribution function) correction based on a modified Walthall model is implemented in XPro. All corrections rely entirely on a priori calibration information and parameters derived from the image data. The details of the correction methods are given by Beisl et al. (2008).

2.6.4   Modified empirical line method. Empirical line method is widely used in reflectance calibration of remote sensing data (Smith and Milton, 1999). In this study a modified version that takes into account the anisotropy of the reference target and uses DNs that are normalized with respect to size of aperture and exposure time was used.

2.6.5   Performance assessment. The performance assessment of radiometric correction is dependent on the type of correction performed.

The validation of methods that carry out reflectance calibration can be related to physical object properties. An estimate of the absolute accuracy is obtained by using accurate enough ground truth reflectance reference targets. In the flight campaigns, artificial reference targets were installed in the area and ground truth measurements were carried out. Repeatability of the reflectance calibration can be evaluated by comparing images collected in repeated acquisitions of same targets from the same or different flying heights. An approximate evaluation of the success of the reflectance calibration can be obtained by evaluating the reflectance spectra of well known targets (asphalt, vegetation). With photogrammetric systems the anisotropy of reflectance has to be taken into account in the analysis.

Quantitative evaluation methods were not available for relative radiometric calibration methods. The radiometric differences between images were visually estimated and the residuals at radiometric tie points were considered. Quantitative criteria for equalization methods could be based on radiometric differences between tie points before and after correction.

2.7 Application oriented studies

The ICC has evaluated the suitability of the DMC data for the NDVI map creation over the entire province of Catalonia.

The suitability of the reflectance calibrated ADS40 data on single tree level species classification was studied by Korpela et al. (2011). They developed a method in which the crown level illumination and occlusion conditions were determined. The method is based on modelling the crown shapes and visibility/shading conditions by using dense LiDAR data. Based on the data, the reflectance characteristics of tree species (within tree species variation, reflectance anisotropy, proximity effects, etc.) were studied in sun illuminated and shadowed conditions. The data with known illumination conditions were then used in further classification experiments by quadratic discriminant analysis (Korpela et al., 2011) and support vector machine classification (Heikkinen et al., 2011).

3. RESULTS AND DISCUSSION

3.1 Radiometric calibration and characterization of the sensor/system

3.1.1 CASI Banyoles. Results by Martinez et al. (2011) indicated that, when CASI smiling effect and CASI spectral sensitivity are taken into account, the atmospheric correction yields fewer artifacts on the atmospherically corrected spectra, even when only standard atmospheric parameters are used. The small artifacts still remaining around the absorption bands could be explained by a frequency dependence of the smiling effect, signal-to-noise ratio too week, etc.

3.1.2 DMC Banyoles. The images were pre-processed as described on the methodology section and afterwards a radiometric calibration was performed through a linear regression for each band and image. Linear relationships with a zero intercept were found for all DMC f-stop values and bands. All the r^2 values obtained were greater than 0.9.

3.1.3 DMC Sjökulla. The results of the vicarious calibration showed that in general the sensor performance was linear; the R^2-values of linear regression were over 0.993. The vicarious calibration was calculated with nine different exposure settings and the radiometric stability of the system was assessed by evaluating the fit of the calibration parameters obtained for one setting with another setting. The difference in R, G and B channels was on average 2.9–4.3% for the same day and the same f-stop data, 3.5–4.5% for the same day and different f-stop data and 3.1−5.2% for data collected on different days. The NIR channel showed weaker performance, and the differences in corresponding cases were 5.7%, 9.2% and 10.9%, respectively. Possible causes of these differences might be sensor instability, inaccuracy of the atmospheric modelling and inaccuracy of the reference values. The stability could be considered to be very good, as it derives from the instabilities of two independent sensors (PAN and MS). Detailed results are given by Markelin et al. (2010a).

3.1.4 ADS40 Hyytiälä. Differences in at-sensor radiances based on the Modtran 4 based at-sensor radiance simulations by ReSe and FGI and the ADS40 processing line were larger than expected (10-20%) (Markelin et al., 2010b; Schläpfer, 2010). Possible causes of differences are on one hand the inaccuracy of reference values and atmospheric modelling in the radiative transfer simulation, and on the other hand possible inaccuracy of the ADS40 laboratory calibration. This issue will be studied further.
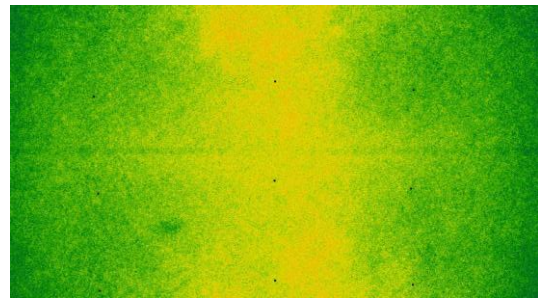

Figure 1. Image sharpness map obtained using 156 images of the Banyoles DMC campaign by the IGN/MATIS. (Brédif and Lelégard, 2010)

3.2 Image data spatial resolution assessment

3.2.1 DMC Banyoles. IGN/MATIS determined the MTFs of the images by using the Siemens star and using a new approach measuring the image sharpness map by the Haar Wavelets (Brédif and Lelégard, 2010). The second method is a potential tool for detection of optical defects and the qualification of the mosaicking of multiple sensor images into a larger composite image. The sharpness map derived from 156 images is shown in Figure 1. The conclusion of the IGN/MATIS evaluations was that the panchromatic photos provided by the DMC camera did not present major defects. The optical system was isotropic and the lens was compatible with the CCD-array (no aliasing). The resolution was better in a centred band parallel to the flight direction.

The ICC used the Siemens star to determine the MTF. The averaged resolution obtained for each image did not show a correlation between the distance to the centre of the image and the resolution. These results are probably due to variables of the acquisition process not taken into account during the study. The histogram of the resolution (FWHM of LSF in pixel units) after implementing a step-like weather simulations for panchromatic channel showed a skewed distribution of resolution values with a large tail towards lower values of resolution (FWHM greater). This distribution indicates that in the majority of cases the resolution is about the maximum frequency, but there are a lot of cases where the atmosphere will produce a large loss of resolution. Besides, there is a high dependence on wavelength, and maximum effect appears at lower wavelengths. These simulation results and the resolution measured in the real DMC panchromatic images are compatible. A more detailed analysis shows that the type and amount of aerosols influence the loss of resolution (Martinez et al., 2009).

3.2.2 DMC Sjökulla. The theoretical expectation regarding the resolution of a DMC image of 12 µm pixel size is 42 line pairs/mm. This theoretical limit for the panchromatic DMC images is decreased due to the convergent image geometry by a factor of up to 1.6 in the image corner. The resolution reached the theoretical expectation in the cross-flight direction at the image center, and was worse by a factor of 1.5 in the furthest image corner; these values are very close to theoretical expectations. The resolution was slightly better in the cross-flight than in the flight direction, which is most likely caused by the forward image motion. The exposure settings (f-stop: 8, 11; exposure time 3.5–6.5 ms) did not influence the resolution. Details of the study are given by Honkavaara et al. (2011).

Figure 2. Banyoles image block Baix/Mig with 42 images corrected by the Pepita software of IGN/ENSG. Top: image mosaic without radiometric correction. Center: Pepita radiometric aerial triangulation with radial component. Bottom: residual values at tie points; highest values are in red and lowest in green. (Chandelier, 2010)

3.3 Reflectance calibration and image block equalization

3.3.1 DMC Banyoles. The Pepita software was used to correct the DMC Banyoles data sets. An example of the equalization results is given in Figure 2. The following conclusions were drawn based on the study (Chandelier, 2010). The solar elevation, exposure time and aperture values were well corrected. The BRDF model worked well especially on forest and agricultural parcels. As expected, the BRDF model did not fit on the lake. In urban areas, the effect of the equalisation was less visible: highest residuals are observed confirming that tie points are not really homologous (a DSM should be used). High residuals occured also in the lake. The radial component didn't improve significantly the equalisation: on the contrary, in urban areas, the radiometric model may not be convergent causing bad equalisation for several images. As a conclusion, Pepita could be used as a tool for relative radiometric calibration for DMC images. To ensure that this result is correct, further testing should be done with additional datasets (more images, different dates…). Performance of the Pepita is fully automatic and it fulfils all the operational requirements of the IGN.

3.3.2 ADS40 Hyytiälä. Reflectance calibration of the Hyytiälä data was carried out by several approaches (Table 1).

XPro was used with atmospheric correction (ATM) and with ATM and BRDF correction. ReSe performed ATCOR-4 processing using Leica's calibration parameters and generic in-flight calibration parameters (retrieved in a different ADS40 campaign); cast shadow correction was tested in the latter case. The FGI carried out ATCOR-4 processing using Leica's laboratory calibration and in-flight calibration parameters derived from the imagery from 2 km and 1 km flying heights.

Figure 3 gives results of the evaluation of the accuracy of the reflectance calibration of an image strip collected from 2 km flying height on good atmospheric conditions (difference to reference value in % of the reflectance). Black target (P05 with nominal reflectance 0.05) and bright targets (P20, P30 and P50 with nominal reflectance 0.20, 0.30, 0.50) were evaluated separately. On bright targets, when in-flight calibration parameters were used, the differences were well below 5% (with a minor exception). If laboratory calibration parameters were used, the differences were clearly higher in blue and NIR channels (7-13%). On black target, when Leica's laboratory calibration was used, differences were 5-20%, depending on the channel; with in-flight calibration the differences were again lower than 5%. When cast shadow correction option of ATCOR-4 was used, large differences (60-120%) appeared on black target; obviously shadow correction has considered black target as a shadow. The accuracy was the best in the case where in-flight calibration parameters from 1 km flying height were used (dark target: better than 5%, bright targets: better than 1.5%).

Markelin et al. (2010b) presented the preliminary results of XPro correction of all flying heights. The results were consistent with above results, indicating that for the evaluated challenging data set, up to 5% reflectance accuracy could be obtained with uniform targets. The accuracy was influenced by the flying height (1-4 km), channel (R, G, B, NIR), level of cloudiness and target properties. An analysis of theoretical basis of the XPro by Heikkinen et al. (2011) showed that the correction is based on planar surfaces and that that the highest

Table 1. Different processing options in ADS40 data reflectance calibration.

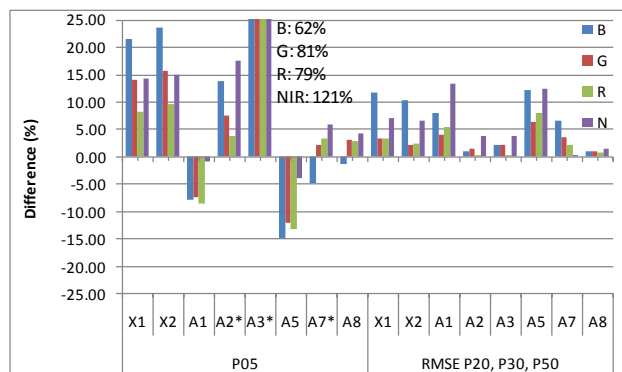|	Method	Calibration	Participant
X1	XPro, ATM	Leica laboratory	FGI
X2	XPro, ATM, BRDF	Leica laboratory	FGI
A1	ATCOR-4	Leica laboratory	ReSe
A2	ATCOR-4	In-flight, 2 km	ReSe
A3	ATCOR-4, Shadows	In-flight, 2 km	ReSe
A5	ATCOR-4	Leica laboratory	FGI
A7	ATCOR-4	In-flight, 2 km	FGI
A8	ATCOR-4	In-flight, 1 km	FGI

Figure 3. Differences of reflectance calibrated ADS40 images to reference targets. *: target was used in calibration.

quality reflectance calibration was possible only in sun illuminated areas. The BRDF correction method is best suited for applications where visually uniform mosaics are of interest. The full comparative results of all data sets (including also data from cloudy conditions) and processing methods will be presented in the final report of the project.

These results are very promising. Issue with very dark targets is that a small error in atmospheric correction leads to large relative error, so larger errors are expected with dark objects. The poorer results in blue channel can be caused by larger atmospheric influences. The results suggest that the laboratory calibrated values might not be accurate enough especially on NIR channel, but also errors in ground truth reflectance values or in atmospheric modelling can cause similar effects. These issues will be studied further.

Swisstopo evaluated the XPro 4.2.0 and ReSe evaluated the ATCOR-4 from the productivity perspective. XPro fulfilled the requirements of the Swisstopo (Bovet, 2010). The evaluation of ATCOR-4 by ReSe showed that the further tuning of software is necessary to fulfil all efficiency and usability requirements of NMAs (Schläpfer, 2010).
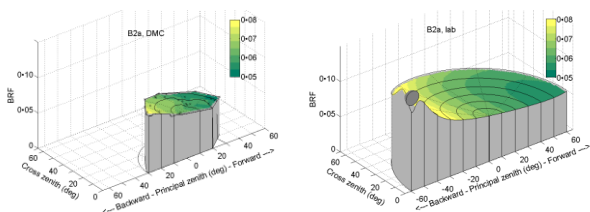

Figure 4. 3D-BRF plot of black gravel measured by the DMC (left) and at laboratory (right). (Honkavaara et al., 2011)

3.3.3   DMC Sjökulla. An empirical line based radiometric correction was carried out with the image block and BRFs of objects in images were provided. A comparison of BRF of black gravel measured in laboratory and from DMC images is shown in Figure 4. The differences of reflectances measured in images to the laboratory calibrated values of independent reference targets were about 5%. This approach does not fulfil productivity requirements of NMAs, but it is functional in small area remote sensing spplications. Detailed results are given by Honkavaara et al. (2011).

3.4 Application oriented analysis

3.4.1   NDVI data sets generation from DMC images. The good results obtained have encouraged ICC to develop an NDVI orthophoto map layer of Catalonia (more than 32,000 km²) during 2011 based on DMC imagery calibrated with using the methodology discussed here. First, the user of this layer will be the Agriculture Department of the Generalitat de Catalunya (regional government) just a few weeks after the flight. Next, a few months later the data will be published. Then, the vegetation layer will be freely disseminated according to ICC data policy.

3.4.2   Tree species classification with ADS40 data. The ADS40 data sets that were reflectance calibrated by the XPro software were used in investigations to develop new methods for tree species classification. Examples of the reflectance values of pine, spruce and birch are shown in Figure 5 as the function of the observer zenith angle (Korpela et al., 2011). If

BRDF correction is not applied a clear brightening towards backward scattering direction appears (Figure 5 upper); the BRDF correction compensated efficiently the BRDF effects (Figure 5 lower), but did not improve the classification results. In general, reflectance variations within species was high (the coefficient of variation was 13-31%). Classification experiments with reflectance calibrated data provided an accuracy of about 75-79% with single ADS40 view and 78-82% with two ADS40 views (Heikkinen et al., 2011). In some cases (the training and classification data from different flight lines) the use of reflectance calibrated data provided better classification results than the at-sensor radiance data.
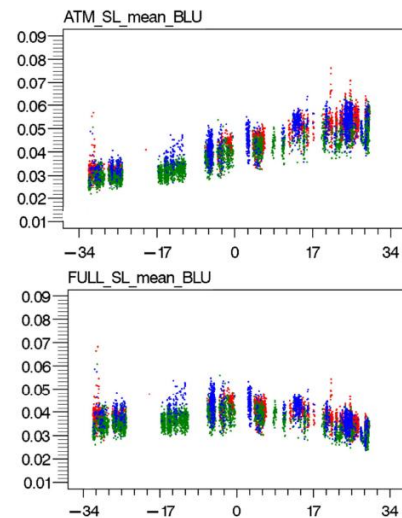

Figure 5. Tree species reflectance in blue channel in the sun lit illumination class as a function of observer zenith angle. Red = pine, green = spruce, blue = birch. Top: atmospheric corrected data. Bottom: BRDF and atmospheric corrected data. (Korpela et al., 2011)

4. CONCLUSIONS

We presented the empirical research carried out for the EuroSDR project "Radiometric aspects of digital photogrammetric images" data sets and provided some highlights of the results. The analysis considered vicarious radiometric calibration, spatial resolution assessment, image block equalization, and reflectance calibration. Furthermore, application oriented studies concerned NDVI layer generation and tree species classification. Data sets were from Leica Geosystems ADS40 and Intergraph DMC and the participants represented stakeholder groups of NMAs, software development and research.

The results proved the stability and quality of the evaluated imaging systems. There are already approaches for reflectance calibration and radiometric equalization of photogrammetric image data that are suited for production environments. The reflectance calibration methods provided up to 5% accuracy without any ground reference targets. For many software products the processing of a whole photogrammetric block is still a limitation. Improvements are also needed in processing of shadowed regions and in treatment of object reflectance anisotropy. It is important to consider the final applications when developing methods for radiometric correction, and on the other hand, the applications (e.g. automatic classification methods) should take into account the level of radiometric correction of the input data.

5. REFERENCES

References from Journals:
Chandelier, L., Martinoty, G, 2009. Radiometric aerial triangulation for the equalization of digital aerial images and orthoimages. Photogrammetric Engineering & Remote Sensing 2009, 75, 193-200.

Fraser, R. S., Ferrare, R. A., Kaufman, Y. J., Markham, B. L., and Mattoo, S., 1992. Algorithm for atmospheric corrections of aircraft and satellite imagery. International Journal of Remote Sensing, 13(3), pp. 541-557.

Heikkinen, V., Korpela, I., Tokola, T., Honkavaara, E., Parkkinen, J., 2011. An SVM classification of tree species radiometric signatures based on the Leica ADS40 sensor. IEEE Trans. Geosci. Remote Sens., In press.

Honkavaara, E., Arbiol, R., Markelin, L., Martinez, L., Cramer, M., Bovet, S., Chandelier, L., Ilves, R., Klonus, S., Marshall, P., Scläpfer, D., Tabor, M., Thom, C., and N. Veje, 2009. Digital airborne photogrammetry – A new tool for quantitative remote sensing? – A state-of-the-art review on radiometric aspects of digital photogrammetric images. Remote Sensing, Vol. 1, 577-605.

Honkavaara, E., Nurminen, K., Markelin, L., Suomalainen, J., Ilves, R., 2011. Calibrating and validating multispectral 3D imaging systems at a permanent test site – Case study with an Intergraph DMC. Photogrammetric Record, In press.

Korpela, I., Heikkinen V., Honkavaara E., Rohrbach F., Tokola T., 2011. Variation and directional anisotropy of reflectance at the crown scale – implications for tree species classification in digital aerial images. Remote Sensing of Environment. In press.

Markelin, L., Honkavaara, E., Hakala, T., Suomalainen and J., Peltoniemi, J., 2010a. Radiometric stability assessment of an airborne photogrammetric sensor in a test field. ISPRS Journal of Photogrammetry and Remote Sensing, 65(4): 409-421.

Markelin, L., Honkavaara, E., Beisl, U. and Korpela, I., 2010b. Validation of the radiometric processing chain of the Leica ADS40 airborne photogrammetric sensor. International Archives of Photogrammetry, Remote Sensing and Spatial Information Sciences, 38(7A): 145-150.

Richter, R., and Schläpfer, D., "Geo-atmospheric processing of airborne imaging spectrometry data. Part 2: atmospheric/topographic correction", Int. J. Remote Sensing 23:2631-2649 (2002).

Smith, G.M.; Milton, E.J, 1999. The use of the empirical line method to calibrate remotely sensed data to reflectance. Remote Sensing 1999, 20, 2653-2662.

Song, J., Lu, D., and Weseley, M. L., 2003. A simplified atmospheric correction procedure for the normalized difference vegetation index. Photogrammetric Engineering & Remote Sensing, 69(5), pp. 521-528.

Suomalainen, J., Hakala, T., Peltoniemi, J., Puttonen, E., 2009. Polarised Multiangular Reflectance Measurements Using the Finnish Geodetic Institute Field Goniospectrometer. Sensors 9 (5), 3891-3907.

Vermote, E.F., Tanré, D., Deuzé, J.L., Herman M., and Morcrette, JJ., 1997. Second simulation of the satellite signal in the solar spectrum, 6S: an overview. IEEE Transactions on Geoscience and Remote Sensing, 35, 675-686, 1997.

References from Other Literature:
Arbiol R., Martinez L., 2009. ICC-Banyoles 2008 Campaign in the framework of EUROSDR Radiometry Project. Project description and preliminary results. International Geomatic Week, Castelldefels (Barcelona) 3 - 5 March.

Beisl, U., Telaar, J., and Schönermark, M. V., 2008. Atmospheric correction, reflectance calibration and BRDF correction for ADS40 image data. In: The International Archives of the Photogrammetry, Remote Sensing and Spatial Information Sciences, Beijing, China, Vol. XXXVII, part B7.

Martínez L., Palà V., Arbiol R and Pérez F., 2007. Digital Metric Camera radiometric and colorimetric calibration with simultaneous CASI imagery to a CIE Standard Observer based colour space. IEEE International Geoscience and Remote Sensing Symposium. Barcelona, 23-27th July.

Martínez, L., Pérez, F., Arbiol, R., Tardà, A., 2011. Radiometric characterisation of a VNIR hyperspectral imaging system for accurate atmospheric correction. International Geomatic Week. 15 – 17 March, Barcelona.

Martinez L., Soler M.E., Pérez F. y Arbiol R., 2009. Efecto de la atmósfera en la resolución de la DMC. XIII Congreso de la Asociación Española de Teledetección. Calatayud (Zaragoza) 23-26 September.

Richter, R: "Atmospheric / Topographic Correction for Airborne Imagery" (2010), DLR report DLR-IB 565-02/10, Wessling, Germany.

Talaya, J., Kornus, W., Alamús, R., Soler, E., Pla, M., Ruiz, A., 2008. Analyzing DMC performance in a production environment XXI ISPRS Congress. Beijing 3-11 July.

References from websites:
EuroSDR, http://www.eurosdr.net/start/

Bovet, S., 2010. Phase2 empirical evaluation of ADS data Product generation with the Hyytiälä dataset at Swisstopo. Project report.

Brédif, M., Lelégard, L., 2010. Study of DMC panchro images resolution. Project report.

Chandelier, L., 2010. Performance test of IGN radiometric aerial triangulation. Project report.

Schläpfer, D., 2010. The Potential of Atmospheric and Topographic Correction for ADS40/80. EuroSDR project report.